Expected Production of Strange Baryons and Antibaryons in Baryon-Poor QGP

Johann Rafelski and Jean Letessier
Department of Physics, University of Arizona, Tucson, AZ 85721, USA
LPTHE, Université Paris 7, 2 place Jussieu, F–75251 Cedex 05
(August 5, 1999)

In a dynamical model of QGP at RHIC we obtain the temporal evolution of strange phase space occupancy at conditions expected to occur in 100+100A GeV nuclear collisions. We show that the sudden QGP break up model developed to describe the SPS experimental results implies dominance of both baryon and antibaryon abundances by the strange baryon and antibaryon yields.

PACS number(s): 12.38.Mh, 25.75.-q

We explore the consequences of high strangeness abundance we expect to be present in the baryon-poor quark-gluon plasma (QGP) environment formed *e.g.*, in the central rapidity region in Au–Au, maximum energy 100+100A GeV collisions at the relativistic heavy ion collider (RHIC) at the Brookhaven National Laboratory, Upton, New York. About 10–20% of hadrons produced in these reactions will be strange, and since mesons dominate hadron abundance, there is much more strangeness than baryon number. During the break-up of the color charge deconfined QGP phase there is considerable advantage for strangeness to stick to baryons given that the energy balance for the same flavor content favors production of strange baryons over kaons, $(E(\Lambda+\pi) < E(\mathrm{N+K}))$. When QGP is formed, we therefore expect to find hyperon dominance of baryon distribution *i.e.* most baryons and antibaryons produced at RHIC will be strange. A similar argument could be made for reactions leading to the confined phase, the main difference arises from the observation that the required high abundance of strangeness per participating nucleon can be produced in the deconfined QGP [1–4]. This qualitative argument will be quantitatively elaborated here, in view of the considerable effort that has been committed by the STAR collaboration at RHIC to enhance the capability to measure multi-strange (anti)baryon production using a silicon strip detector (SSD) [5].

In the first part of this report we show that the chemical strangeness flavor abundance equilibrium is established at the time of QGP breakup by the dominant process which is gluon fusion, $GG \to s\bar{s}$. In QGP this reaction overcomes the current quark mass threshold $2m_{\mathrm{s}}$ for strangeness formation for temperature $T \simeq m_{\mathrm{s}} > 200\,\mathrm{MeV}$. In the second part of this report we use the computed chemical condition of strangeness, and employ the knowledge gained in our analysis of the SPS results [6], to obtain the strange baryon and antibaryon abundances expected at RHIC.

In some key aspects the methods we employ differ from those obtained in other studies of chemical equilibration of quark flavor for RHIC conditions [7–9]. We study the dynamics of the phase space occupancy rather than particle density, and we eliminate most of the dynamical flow effects by considering entropy conserving evolution. Moreover, we use running QCD parameters (both coupling and strange quark mass) to describe strangeness production, with strong coupling constant α_s as determined at the M_{Z^0} energy scale. We will make two assumptions of relevance for the results we obtain:
a) the kinetic (momentum distribution) equilibrium is reached faster than the chemical (abundance) equilibrium [10,11];
b) gluons equilibrate chemically significantly faster than strangeness [12].
The first assumption allows to study only the chemical abundances, rather than the full momentum distribution, which simplifies greatly the structure of the master equations; the second assumption allows to focus after an initial time τ_0 has passed on the evolution of strangeness population: τ_0 is the time required for the development to near chemical equilibrium of the gluon population.

We now formulate the dynamical equation for the evolution of the phase space occupancy γ_{s} of strange quarks in the expanding QGP: the phase space distribution f_{s} can be characterized by a local temperature $T(\vec{x},t)$ of a (Boltzmann) equilibrium distribution f_{s}^{∞}, with normalization set by a phase space occupancy factor:

$$f_{\mathrm{s}}(\vec{p},\vec{x};t)) \simeq \gamma_{\mathrm{s}}(T) f_{\mathrm{s}}^{\infty}(\vec{p};T)\,. \tag{1}$$

Eq. (1) invokes in the momentum independence of γ_{s} our first assumption. More generally, the factor γ_i, $i = g,q,s,c$ allows a local density of gluons, light quarks, strange quarks and charmed quarks, respectively not to be determined by the local momentum shape, but to evolve independently.

With variables $(t,\vec{x})$ referring to an observer in the laboratory frame, the chemical evolution can be described by the strange quark current non-conservation arising from strange quark pair production described by a Boltzmann collision term:

$$\partial_\mu j^\mu_{\mathrm{s}} \equiv \frac{\partial \rho_{\mathrm{s}}}{\partial t} + \frac{\partial \vec{v}\rho_{\mathrm{s}}}{\partial \vec{x}} = \frac{1}{2}\rho_g^2(t)\,\langle\sigma v\rangle_T^{gg\to s\bar{s}} + \\ + \rho_q(t)\rho_{\bar{q}}(t)\langle\sigma v\rangle_T^{q\bar{q}\to s\bar{s}} - \rho_{\mathrm{s}}(t)\,\rho_{\bar{\mathrm{s}}}(t)\,\langle\sigma v\rangle_T^{s\bar{s}\to gg,q\bar{q}}. \tag{2}$$

The factor 1/2 avoids double counting of gluon pairs. The implicit sums over spin, color and any other discreet quantum numbers are combined in the particle density $\rho = \sum_{s,c,\ldots} \int d^3p\, f$, and we have also introduced the momentum averaged production/annihilation thermal reactivities:

$$\langle \sigma v_{\rm rel} \rangle_T \equiv \frac{\int d^3p_1 \int d^3p_2 \sigma_{12} v_{12} f(\vec{p}_1,T) f(\vec{p}_2,T)}{\int d^3p_1 \int d^3p_2 f(\vec{p}_1,T) f(\vec{p}_2,T)} \,. \quad (3)$$

$f(\vec{p}_i,T)$ are the relativistic Boltzmann/Jüttner distributions of two colliding particles $i = 1,2$ of momentum p_i.

The current conservation can also be written with reference to the individual particle dynamics [13]: consider $\rho_{\rm s}$ as the inverse of the small volume available to each particle. Such a volume is defined in the local frame of reference for which the local flow vector vanishes $\vec{v}(\vec{x},t)|_{\rm local} = 0$. The considered volume δV_l being occupied by small number of particles δN (*e.g.*, $\delta N = 1$), we have:

$$\delta N_{\rm s} \equiv \rho_{\rm s} \delta V_l \,. \quad (4)$$

The left hand side (LHS) of Eq. (2) can be now written as:

$$\frac{\partial \rho_{\rm s}}{\partial t} + \frac{\partial \vec{v} \rho_{\rm s}}{\partial \vec{x}} \equiv \frac{1}{\delta V_l} \frac{d \delta N_{\rm s}}{dt} = \frac{d\rho_{\rm s}}{dt} + \rho_{\rm s} \frac{1}{\delta V_l} \frac{d \delta V_l}{dt} \,. \quad (5)$$

Since δN and $\delta V_l dt$ are L(orentz)-invariant, the actual choice of the frame of reference in which the right hand side (RHS) of Eq. (5) is studied is irrelevant and we drop henceforth the subscript l.

We can further adapt Eq. (5) to the dynamics we pursue: we introduce $\rho_{\rm s}^\infty(T)$ as the (local) chemical equilibrium abundance of strange quarks, thus $\rho = \gamma_{\rm s} \rho_{\rm s}^\infty$. We evaluate the equilibrium abundance $\delta N_{\rm s}^\infty = \delta V \rho_{\rm s}^\infty(T)$ integrating the Boltzmann distribution:

$$\delta N_{\rm s}^\infty = [\delta V T^3] \frac{3}{\pi^2} z^2 K_2(z) \,, \quad z = \frac{m_{\rm s}}{T} \,, \quad (6)$$

where K_ν is the modified Bessel function of order ν; we will below use: $d[z^\nu K_\nu(z)]/dz = -z^\nu K_{\nu-1}$. The first factor on the RHS in Eq. (6) is a constant in time should the evolution of matter after the initial pre-thermal time period τ_0 be entropy conserving [14], and thus $\delta V T^3 = \delta V_0 T_0^3$=Const.. We now substitute in Eq. (5) and obtain

$$\frac{\partial \rho_{\rm s}}{\partial t} + \frac{\partial \vec{v} \rho_{\rm s}}{\partial \vec{x}} = \dot{T} \rho_{\rm s}^\infty \left(\frac{d\gamma_{\rm s}}{dT} + \frac{\gamma_{\rm s}}{T} z \frac{K_1(z)}{K_2(z)} \right) \,, \quad (7)$$

where $\dot{T} = dT/dt$. Note that in Eq. (7) only a part of the usual flow-dilution term is left, since we implemented the adiabatic volume expansion, and study the evolution of the phase space occupancy in lieu of particle density. The dynamics of the local temperature is the only quantity we need to model.

We now return to study the collision terms seen on the RHS of Eq. (2). A related quantity is the (L-invariant) production rate $A^{12\to 34}$ of particles per unit time and space, defined usually with respect to chemically equilibrated distributions:

$$A^{12\to 34} \equiv \frac{1}{1+\delta_{1,2}} \rho_1^\infty \rho_2^\infty \langle \sigma_{\rm s} v_{12} \rangle_T^{12\to 34} \,. \quad (8)$$

The factor $1/(1+\delta_{1,2})$ is introduced to compensate double-counting of identical particle pairs. In terms of the L-invariant A, Eq. (2) takes the form:

$$\dot{T} \rho_{\rm s}^\infty \left(\frac{d\gamma_{\rm s}}{dT} + \frac{\gamma_{\rm s}}{T} z \frac{K_1(z)}{K_2(z)} \right) = \gamma_g^2(\tau) A^{gg\to s\bar{s}} + \\ + \gamma_q(\tau)\gamma_{\bar{q}}(\tau) A^{q\bar{q}\to s\bar{s}} - \gamma_{\rm s}(\tau)\gamma_{\bar{s}}(\tau)(A^{s\bar{s}\to gg} + A^{s\bar{s}\to q\bar{q}}). \quad (9)$$

Only weak interactions convert quark flavors, thus, on hadronic time scale, we have $\gamma_{s,q}(\tau) = \gamma_{\bar{s},\bar{q}}(\tau)$. Moreover, detailed balance, arising from the time reversal symmetry of the microscopic reactions, assures that the invariant rates for forward/backward reactions are the same, specifically

$$A^{12\to 34} = A^{34\to 12}, \quad (10)$$

and thus:

$$\dot{T} \rho_{\rm s}^\infty \left(\frac{d\gamma_{\rm s}}{dT} + \frac{\gamma_{\rm s}}{T} z \frac{K_1(z)}{K_2(z)} \right) = \gamma_g^2(\tau) A^{gg\to s\bar{s}} \left[1 - \frac{\gamma_{\rm s}^2(\tau)}{\gamma_g^2(\tau)} \right] \\ + \gamma_q^2(\tau) A^{q\bar{q}\to s\bar{s}} \left[1 - \frac{\gamma_{\rm s}^2(\tau)}{\gamma_q^2(\tau)} \right] \,. \quad (11)$$

When all $\gamma_i \to 1$, the Boltzmann collision term vanishes, we have reached equilibrium.

As discussed, the gluon chemical equilibrium is thought to be reached at high temperatures well before the strangeness equilibrates chemically, and thus we assume this in what follows, and the initial conditions we will study refer to the time at which gluons are chemically equilibrated. Setting $\lambda_g = 1$ (and without a significant further consequence for what follows, since gluons dominate the production rate, also $\lambda_q = 1$) we obtain after a straightforward manipulation the dynamical equation describing the evolution of the local phase space occupancy of strangeness:

$$2\tau_{\rm s} \dot{T} \left(\frac{d\gamma_{\rm s}}{dT} + \frac{\gamma_{\rm s}}{T} z \frac{K_1(z)}{K_2(z)} \right) = 1 - \gamma_{\rm s}^2 \,. \quad (12)$$

Here, we defined the relaxation time $\tau_{\rm s}$ of chemical (strangeness) equilibration as the ratio of the equilibrium density that is being approached, with the rate at which this occurs:

$$\tau_{\rm s} \equiv \frac{1}{2} \frac{\rho_{\rm s}^\infty}{(A^{gg\to s\bar{s}} + A^{q\bar{q}\to s\bar{s}} + \ldots)} \,. \quad (13)$$

The factor 1/2 is introduced by convention in order for the quantity $\tau_{\rm s}$ to describe the exponential approach to equilibrium.

Eq. (12) is our final analytical result describing the evolution of phase space occupancy. Since one generally expects that $\gamma_s \to 1$ in a monotonic fashion as function of time, it is important to appreciate that this equation allows $\gamma_{\rm s} > 1$: when T drops below $m_{\rm s}$, and $1/\tau_{\rm s}$ becomes small, the dilution term (2nd term on LHS) in Eq. (12) dominates the evolution of $\gamma_{\rm s}$. In simple terms, the high abundance of strangeness produced at high temperature over-populates the available phase space at lower temperature, when the equilibration rate cannot keep up with the expansion cooling. This behavior of $\gamma_{\rm s}$ has been shown in Fig. 2 of Ref [15] for the SPS conditions with fast transverse expansion. Since we assume that the dynamics of transverse expansion of QGP is similar at RHIC as at SPS, we will obtain a rather similar behavior for $\gamma_{\rm s}$. We note that yet a faster transverse expansion than considered here could enhance the chemical strangeness anomaly.

$\tau_{\rm s}(T)$, Eq. (13), has been evaluated using pQCD cross section and employing NLO (next to leading order) running of both the strange quark mass and QCD-coupling constant α_s [16]. We believe that this method produces a result for α_s that can be trusted down to 1 GeV energy scale which is here relevant. We employ results obtained with $\alpha_s(M_{Z^0}) = 0.118$ and $m_{\rm s}(1{\rm GeV}) = 220\,{\rm MeV}$, a somewhat conservative (high) choice for $m_{\rm s}$, which should under-predict strangeness production. There is some systematic uncertainty due to the appearance of the strange quark mass as a fixed rather than running value in both, the chemical equilibrium density $\rho_{\rm s}^{\infty}$ in Eq. (13), and in the dilution term in Eq. (12). We use the value $m_{\rm s}(1\,{\rm GeV})$, with the energy scale chosen to correspond to typical interaction scale in the QGP.

Numerical study of Eq. (12) becomes possible as soon as we define the temporal evolution of the temperature for RHIC conditions. We expect that a global cylindrical expansion should describe the dynamics: aside of the longitudinal flow, we allow the cylinder surface to expand given the internal thermal pressure. SPS experience suggests that the transverse matter flow will not exceed the sound velocity of relativistic matter $v_\perp \simeq c/\sqrt{3}$. We recall that for pure longitudinal expansion local entropy density scales as $S \propto T^3 \propto 1/\tau$, [14]. It is likely that the transverse flow of matter will accelerate the drop in entropy density. We thus consider the following temporal evolution function of the temperature:

$$T(\tau) = T_0 \left[\frac{1}{(1+\tau\ 2c/d)(1+\tau\ v_\perp/R_\perp)^2} \right]^{1/3} . \qquad (14)$$

We take the thickness of the initial collision region at $T_0 = 0.5\,{\rm GeV}$ to be $d(T_0 = 0.5)/2 = 0.75\,{\rm fm}$, and the transverse dimension in nearly central Au–Au collisions to be $R_\perp = 4.5\,{\rm fm}$. The time at which thermal initial conditions are reached is assumed to be $\tau_0 = 1{\rm fm}/c$. When we vary T_0, the temperature at which the gluon equilibrium is reached, we also scale the longitudinal dimension according to:

$$d(T_0) = (0.5\,{\rm GeV}/T_0)^3 1.5\,{\rm fm}\,. \qquad (15)$$

This assures that when comparing the different evolutions of γ_s we are looking at an initial system that has the same entropy content. The reason we vary the initial temperature T_0 down to 300 MeV, maintaining the initial entropy content is to understand how the assumption about the chemical equilibrium of gluons, reached by definition at T_0, impacts our result.

The numerical integration of Eq. (12) is started at τ_0, and a range of initial temperatures $300 \le T_0 \le 600$, varying in steps of 50 MeV. The high limit of the temperature we explore exceeds somewhat the "hot glue scenario" [10], while the lower limit of T_0 corresponds to the more conservative estimates of possible initial conditions [14]. Since the initial p–p collisions also produce strangeness, we take as an estimate of initial abundance a common initial value $\gamma_{\rm s}(T_0) = 0.2$. The time evolution in the plasma phase is followed up to the break-up of QGP. This condition we establish in view of our analysis of the SPS results. We recall that SPS-analysis showed that the system dependent baryon and antibaryon $m_\perp$-slopes of particle spectra are result of differences in collective flow in the deconfined QGP source at freeze-out [6]. There is a universality of physical properties of hadron chemical freeze-out between different SPS systems, and in our analysis a practical coincidence of the kinetic freeze-out conditions with the chemical freeze-out. We thus expect extrapolating the phase boundary curve to the small baryochemical potentials that the QGP break-up temperature $T_f^{\rm SPS} \simeq 145 \pm 5$ MeV will see just a minor upward change to the value $T_f^{\rm RHIC} \simeq 150 \pm 5$ MeV.

With the freeze-out condition fixed, one would think that the major uncertainty in our approach comes from the initial gluon equilibration temperature T_0, and we now study how different values of T_0 influence the final state phase space occupancy. We integrate numerically Eq. (12) and present $\gamma_{\rm s}$ as function of both time t in Fig. 1a, and temperature T in Fig. 1b, up to the expected QGP breakup at $T_f^{\rm RHIC} \simeq 150 \pm 5$ MeV. We see that:

- widely different initial conditions (with similar initial entropy content) lead to rather similar chemical conditions at chemical freeze-out of strangeness,
- despite a series of conservative assumptions we find not only that strangeness equilibrates, but indeed that the dilution effect allows an overpopulation of the strange quark phase space. For a wide range of initial conditions we obtain a narrow band $1.18 > \gamma_{\rm s}(T_f) > 0.95$. We will in the following study of strange baryon and antibaryon abundances adopt what we believe to be the most likely value $\gamma_{\rm s}(T_f) = 1.15$.

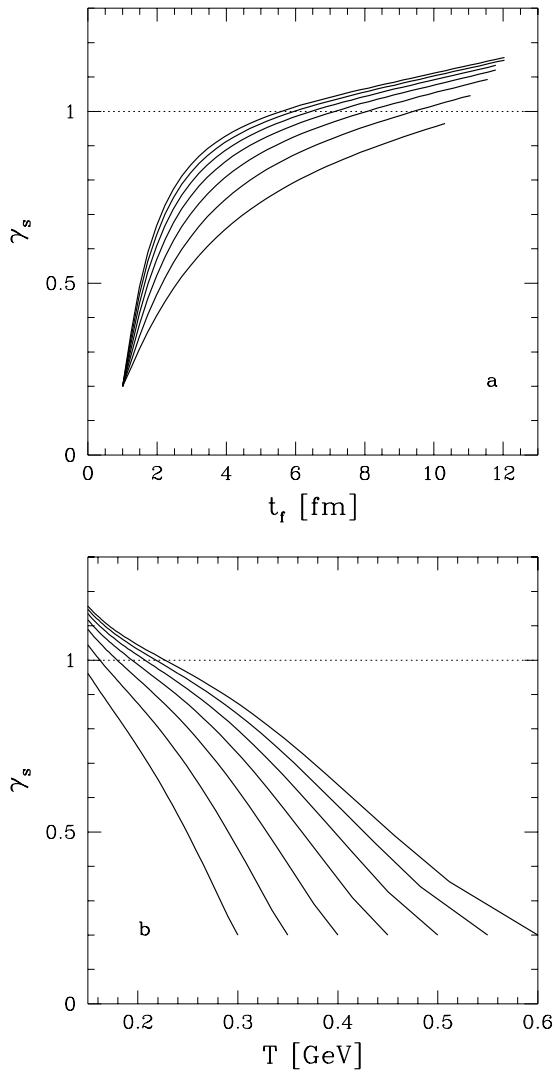

FIG. 1. Evolution of QGP-phase strangeness phase space occupancy γ_s **a**) as function of time and **b**) as function of temperature, see text for details.

We now consider how this relatively large value of γ_s, characteristic for the underlying QGP formation and evolution of strangeness, impacts the strange baryon and anti-baryon observable emerging in hadronization. Remembering that major changes compared to SPS should occur in rapidity spectra of mesons, baryons and antibaryons, we will apply the same hadronization model that worked in the analysis of the SPS data [6]:
1) the QGP freeze-out/break-up occurs without a significant (transient) hadronic gas epoch;
2) the deconfined QGP state evaporates over a few fm/c, during which time it remains near to the freeze-out temperature, with energy lost due to particle evaporation and work done against the vacuum balanced by the internal energy flows. This reaction picture can be falsified easily, since we expect, based and compared to the Pb–Pb 158A GeV results:
a) shape identity of RHIC $m_\perp$ and y spectra of antibaryons $\bar{p}$, $\overline{\Lambda}$, $\overline{\Xi}$, since in our approach there is no difference in their production mechanism, and the form of the spectra is determined in a similar way by the local temperature and flow velocity vector;
b) the $m_\perp$-slopes of these antibaryons should be very similar to the result we have from Pb–Pb 158A GeV since only a slight increase in the freeze-out temperature occurs, and no increase in collective transverse flow is expected.

The abundances of particles produced from QGP within this sudden freeze-out model are controlled by several further chemical parameters: the light quark fugacity $1 < \lambda_q < 1.1$, value is limited by the expected small ratio between baryons and mesons (baryon-poor plasma) when the energy per baryon is above 100 GeV, strangeness fugacity $\lambda_s \simeq 1$ which value for locally neutral plasma assures that $\langle s - \bar{s} \rangle = 0$; the light quark phase space occupancy $\gamma_q \simeq 1.5$, overabundance value due to gluon fragmentation. Given these narrow ranges of chemical parameters and the freeze-out temperature $T_f = 150$ MeV, we compute the expected particle production at break-up. In general we cannot expect that the absolute numbers of particles we find are correct, as we have not modeled the important effect of flow in the laboratory frame of reference. However, ratios of hadrons subject to similar flow effects (compatible hadrons) can be independent of the detailed final state dynamics, as the results seen at SPS suggest [6], and we will look at such ratios more closely.

Taking $\gamma_q = 1.25, 1.5, 1.6$ we choose the value of λ_q, see the header of table I, for which the energy per baryon (E/b) is similar to the collision condition (100 GeV), which leads here to the range $\lambda_q = 1.03 \pm 0.005$. We evaluate for these examples aside of E/b, the strangeness per baryon s/b and entropy per baryon S/b as shown in the top section of the table I. We do not enforce $\langle s - \bar{s} \rangle = 0$ exactly, but since baryon asymmetry is small, strangeness is balanced to better than 2% in the parameter range considered. In the bottom portion of table I we present the compatible particle abundance ratios, computed according to the procedure developed in [6]. We have presented aside of the baryon and antibaryon relative yields also the relative kaon yield, which is also well determined within our approach.

The meaning of these results can be better appreciated when we assume in an example the central rapidity density of protons is $dp/dy|_{\rm central} = 25$. In table II we present the resulting (anti)baryon abundances. We see that the net baryon density $db/dy \simeq 15 \pm 2$, there is baryon number transparency. We see that (anti)hyperons are indeed more abundant than non-strange (anti)baryons. It is important when quoting results from table II to recall that:
1) we have chosen arbitrarily the overall normalization in table II, only particle ratios were computed, and
2) the rapidity baryon density relation to rapidity pro-

ton density is a consequence of the assumed value of λ_q, which we chose to get $E/b \simeq 100\,\mathrm{GeV}$ per participant.

However, we firmly believe that our key result seen in table II , the hyperon-dominance of the baryon yields, does not depend on these hypothesis. Indeed, we have explored another set of parameters in our first and preliminary report on this matter [17], finding the same primary conclusion explained in the introduction. Another related notable result, seen in table I, is that strangeness yield per participant is 13–23 times greater than seen at present at SPS energies, where we have 0.75 strange quark pairs per baryon. As seen in table II the baryon rapidity density is in our examples similar to the proton rapidity density.

In summary, we have shown that one can expect strangeness chemical equilibration in nuclear collisions at RHIC if the deconfined QGP is formed, with a probable overpopulation effect associated with the early strangeness abundance freeze-out before hadronization. We studied the physical conditions at QGP breakup and have shown that (anti)hyperons dominate (anti)baryon abundance.

Acknowledgments: This work was supported in part by a grant from the U.S. Department of Energy, DE-FG03-95OR40937. LPTHE, Univ. Paris 6 et 7 is: Unité mixte de Recherche du CNRS, UMR7589.

[1] J. Rafelski and B. Müller, *Phys. Rev. Lett* **48**, 1066 (1982); **56**, 2334E (1986);
P. Koch, B. Müller and J. Rafelski, *Z. Phys.* A **324**, 453 (1986).

[2] T. Matsui, B. Svetitsky and L.D. McLerran, *Phys. Rev.* D **34**, 783 and 2047 (1986).

[3] N. Bilic, J. Cleymans, I. Dadic and D. Hislop, *Phys. Rev.* C **52**, 401 (1995).

[4] J. Rafelski, J. Letessier and A. Tounsi, *Acta Phys. Pol.* B **27**, 1037 (1996).

[5] *Proposal for a Silicon Strip Detector for STAR* a SUBATECH-Nantes, France led STAR project.
Compare also STAR collaboration web page:
http://www.star.bnl.gov/star/starlib/doc/www/html/strange_l/strange.html

[6] J. Rafelski and J. Letessier, "Hadrons from Pb–Pb collisions at 158*A* GeV", nucl-th/9903018; J. Letessier and J. Rafelski, *Phys. Rev.* **C 59** (1999) 947; *Acta Phys. Pol.*, **B 30** (1999) 153; *J. Phys.*, **G 25** (1999) 295.

[7] T.S. Biró, E. van Doorn, B. Müller, M.H. Thoma and X.-N. Wang, *Phys. Rev.* C **48**, 1275 (1993).

[8] S.M.H. Wong, *Phys. Rev.* C **54**, 2588 (1996); and **56**, 1075 (1996), and references therein.

[9] D.K. Srivastava, M.G. Mustafa and B. Müller, *Phys. Lett.* B **396**, 45 (1997); *Phys. Rev.* C **56**, 1054 (1997).

[10] E. Shuryak, *Phys. Rev. Lett.* **68**, 3270 (1992).

[11] Jan-e Alam, S. Raha and B. Sinha, *Phys. Rev. Lett.* **73**, 1895 (1994);
P. Roy, Jan-e Alam, S. Sarkar, B. Sinha, and S. Raha, *Nucl. Phys.* A **624**, 687 (1997).

[12] S.M.H. Wong *Phys. Rev.* C **56**, 1075 (1997).

[13] The conventional "Eulerian" formulation of Hydrodynamics and its relation to the "Lagrangian" description here required is discussed in older texts such as:
H. Lamb, *Hydrodynamics* Dover Publications (New York) reprint of Cambridge University Press 6th edition (1932).

[14] J.D. Bjorken, *Phys. Rev.* D **27**, 140 (1983).

[15] J. Letessier, A. Tounsi and J. Rafelski, *Phys. Lett.* B **390**, 363 (1997).

[16] J. Rafelski, J. Letessier and A. Tounsi, *APH N.S., Heavy Ion Physics*, **4**, 181 (1996);
J. Letessier, J. Rafelski, and A. Tounsi, *Phys. Lett.* B **389**, 586 (1996).

[17] http://www.qm99.to.infn.it/program/qmprogram.html Presentation on Friday, May 24, 1999 at 11:25AM by J. Rafelski; to appear in proceedings of *Quark Matter 1999*, Torino, Italy within a group report "*Last call for* RHIC *predictions*". S. Bass *et. al.*, nucl-th/9907090.

TABLE I. For $\gamma_\mathrm{s} = 1.15$, $\lambda_\mathrm{s} = 1$ and γ_q, λ_q as shown: Top portion: strangeness per baryon s/b, energy per baryon E/b[GeV] and entropy per baryon S/b. Bottom portion: sample of hadron ratios expected at RHIC.

γ_q	1.25	1.5	1.5	1.5	1.60
λ_q	1.03	1.025	1.03	1.035	1.03
E/b[GeV]	117	133	111	96	110
s/b	17	15	12	11	11
S/b	623	693	579	497	567
$p/\bar{p}$	1.19	1.15	1.19	1.22	1.19
Λ/p	1.61	1.35	1.35	1.34	1.25
$\bar{\Lambda}/\bar{p}$	1.71	1.41	1.42	1.43	1.33
$\bar{\Lambda}/\Lambda$	0.89	0.91	0.89	0.87	0.89
Ξ/Λ	0.17	0.146	0.145	0.145	0.13
$\overline{\Xi}/\bar{\Lambda}$	0.18	0.15	0.15	0.15	0.14
$\overline{\Xi}/\Xi$	0.94	0.95	0.94	0.93	0.94
Ω/Ξ	0.135	0.114	0.113	0.112	0.106
$\overline{\Omega}/\overline{\Xi}$	0.144	0.119	0.120	0.121	0.113
$\overline{\Omega}/\Omega$	1	1.	1.	1.	1.
$\frac{(\Omega+\overline{\Omega})}{(\Xi+\bar{\Xi})}$	0.14	0.12	0.12	0.12	0.11
$\frac{(\Xi+\bar{\Xi})}{(\Lambda+\bar{\Lambda})}$	0.18	0.15	0.15	0.15	0.14
K^+/K^-	1.05	1.04	1.05	1.06	1.05

TABLE II. $dN/dy|_\mathrm{central}$ assuming in this example $dp/dy|_\mathrm{central} = 25$.

γ_q	λ_q	b	p	$\bar{p}$	$\Lambda{+}\Sigma^0$	$\overline{\Lambda}{+}\overline{\Sigma}^0$	$\Sigma^\pm$	$\overline{\Sigma}^\pm$	Ξ	$\overline{\Xi}$	$\Omega{=}\overline{\Omega}$
1.25	1.03	16	25*	21	40	36	28	25	14	13	0.9
1.5	1.025	13	25*	22	34	31	24	21	11	9.4	0.6
1.5	1.03	15	25*	21	34	30	24	21	9.8	9.2	0.6
1.5	1.035	17	25*	21	33	29	23	20	9.6	9.0	0.5
1.60	1.03	14	25*	21	31	28	22	19	8.6	8.0	0.5